

CONTINUAL LOW-RANK ADAPTERS FOR LLM-BASED GENERATIVE RECOMMENDER SYSTEMS

Hyunsik Yoo¹, Ting-Wei Li¹, SeongKu Kang², Zhining Liu¹,
Charlie Xu³, Qilin Qi³, Hanghang Tong¹

¹University of Illinois Urbana–Champaign ²Korea University ³Amazon

hy40@illinois.edu

ABSTRACT

While large language models (LLMs) achieve strong performance in recommendation, they face challenges in continual learning as users, items, and user preferences evolve over time. Existing LoRA-based continual methods primarily focus on preserving performance on previous tasks, but this overlooks the unique nature of recommendation: the goal is not to predict past preferences, and outdated preferences can even harm performance when current interests shift significantly. To address this, we propose PESO (Proximally Eregularized Single evolving lORA), a continual adaptation method for LoRA in recommendation. PESO introduces a proximal regularizer that anchors the current adapter to its most recent frozen state, enabling the model to flexibly balance adaptation and preservation, and to better capture recent user behaviors. Theoretically, we show that this proximal design provides data-aware, direction-wise guidance in the LoRA subspace. Empirically, PESO consistently outperforms existing LoRA-based continual learning methods.

1 INTRODUCTION

Large language models (LLMs) are increasingly used for recommendation by treating the task as sequence generation: given a user’s interaction history, the model autoregressively generates the next item tokens (Bao et al., 2025; Cao et al., 2024; Tan et al., 2024; Wang et al., 2024; Bao et al., 2023; Kweon et al., 2025; Lin et al., 2025). In practice, LLM is fine-tuned on user histories paired with their next interactions, aligning it with the recommendation objective. However, real-world interaction data are continuously collected and evolve over time: new users and items appear, and user preferences drift. Periodic retraining from scratch on both historical and new data is possible but highly inefficient, making *continual learning* (i.e., updating the model effectively with new data) a natural and appealing solution.

It is well known that a continual model must balance *stability* (retaining past knowledge) and *plasticity* (adapting to new knowledge) (Zhu et al., 2021; Arani et al., 2022; Ye et al., 2022; Zhang et al., 2024a; Yuan et al., 2021; Do & Lauw, 2023; Mi et al., 2020). However, continual recommender systems present unique interpretations of these concepts, and bear subtle but critical difference from other domains such as computer vision. In most other domains, continual tasks are typically disjoint and not time-ordered (e.g., cats vs. dogs → trucks vs. sedans), and the primary objective is to preserve performance on previous tasks (stability) while adapting to new ones (plasticity). In contrast, the ultimate goal of continual recommendation is to accurately capture evolving user preferences in order to predict which items a user *will* prefer in the near future. That is, recommendation is not concerned with predicting past user preferences; in fact, outdated preferences can even hinder performance if current user interests have shifted significantly (e.g., a user starts preferring romance over action). Thus, stability in recommendation refers to preserving long-term

user preferences (e.g., enduring interests in certain genres or brands) that remain predictive, even if they are not strongly reflected in recent data. Plasticity, on the other hand, is required to overwrite outdated preferences and to capture emerging trends. This distinct setting in turn requires careful model design.

A common recipe for fine-tuning LLMs in recommendation is Low-Rank Adaptation (LoRA) (Hu et al., 2022; Liu et al., 2025), due to its simplicity and modularity across components (e.g., attention layers). LoRA freezes pretrained weights and injects lightweight, trainable low-rank matrices. This efficiency makes LoRA a natural candidate for continual learning, motivating our focus on continual LoRA for LLM-based recommender systems. A simple and intuitive approach is to maintain a *single evolving LoRA*: sequentially fine-tuning one adapter, initializing it from the previous stage and optimizing it on new data. This provides strong plasticity, while parameter inheritance provides partial preservation of past knowledge. However, it inevitably overwrites useful past knowledge during fine-tuning, leading to forgetting.

To mitigating forgetting, several works in vision have proposed the family of *cumulative LoRA* (Wu et al., 2025; Liang & Li, 2024; Lu et al., 2024), which typically use the sum of the new trainable adapter and all frozen past adapters. This design explicitly enhances stability by reusing prior adapters and expanding LoRA’s effective capacity, and it works well when tasks are largely independent (i.e., with minimal interference), allowing each adapter to encode task-specific knowledge. Intuitively, this might seem beneficial for recommendation, where preserving useful past preferences matters. However, our analysis shows that cumulative LoRA often underperforms the simpler single evolving LoRA. Unlike vision tasks, recommendation involves reappearing users with continuously evolving preferences. The model must therefore capture useful interference across stages, but frozen adapters entangle outdated and relevant preferences, making them hard to disentangle. In addition, as adapters accumulate over time, cumulative LoRA incurs growing storage costs and struggles to reflect their relative importance during aggregation.

To address these limitations, we adopt two principles: (1) avoid multiple adapters, which implicitly assume task independence, and (2) preserve past knowledge in a way that supports understanding of current user behavior. Guided by this, we propose PESO (Proximally regularized Single evolving loRA), which maintains a single evolving LoRA adapter while regularizing it toward its past state with a lightweight proximal term. Unlike cumulative LoRA, PESO balances stability and plasticity through the natural competition between the data-fitting loss and the proximal term, allowing the model to decide what to adapt or retain. Theoretically, we show that this design yields data-aware, direction-wise guidance in the LoRA subspace. We further instantiate it with a per-module softmax–Kullback–Leibler (KL) proximal, which preserves internal module structure rather than treating all parameters equally (i.e., a more nuanced stability mechanism). Empirically, PESO consistently outperforms both cumulative LoRA and the single evolving adapter across multiple real-world datasets, achieving a more effective stability–plasticity balance for recommendation.

In summary, our main contributions are threefold. **(1) Analysis:** we identify the distinctive stability–plasticity challenge in continual recommendation and show empirically that cumulative LoRA, while effective in simulated user-disjoint settings, underperforms in the natural case where user preferences evolve across time stages; **(2) Method and Theory:** we propose PESO, a *proximally regularized LoRA* that anchors each update to the previous state, with theory showing direction-wise, data-aware guidance and a per-module softmax–KL instantiation; **(3) Experiments:** we demonstrate through extensive experiments on real-world datasets that PESO consistently outperforms both single evolving and cumulative LoRA.

2 PRELIMINARY

Notations. We consider an LLM-based recommender that, given a user’s interaction history, autoregressively predicts the next item token. At time stage $t \in \{1, \dots, T\}$, let \mathcal{U}_t be the set of active users, \mathcal{I}_t the set of items, and $\mathcal{E}_t = \{x_u\}_{u \in \mathcal{U}_t}$ the collection of user sequences, where $x_u = (x_{u,1}, \dots, x_{u,N_u})$. Training uses next-item pairs induced from \mathcal{E}_t , yielding state- t data \mathcal{D}_t :

$$\mathcal{D}_t = \{(x_u, y_u) : u \in \mathcal{U}_t\}, \quad y_u = x_{u,N_u+1} \in \mathcal{I}_t. \quad (1)$$

Each item $x_{u,i}$ (and y_u) is represented by *semantic ID* obtained by a codebook-based tokenizer (e.g., RQ-VAE (Rajput et al., 2023)) trained on item semantic features (e.g., title/description), yielding fixed number of token IDs for each item. Semantic ID captures hierarchical semantics of items and works well in practice.¹

Stability and Plasticity in Continual Recommendation. We assume an initial model is pre-trained offline on base data \mathcal{D}_1 , and then fine-tuned sequentially on chronologically arriving blocks $\mathcal{D}_2, \dots, \mathcal{D}_T$. The goal of continual recommendation is to minimize expected risk on upcoming interactions by balancing *stability* (retaining persistent long-term preferences) and *plasticity* (adapting to new or shifting preferences from recent data), thereby capturing evolving user interests (see Appendix A for a formal conceptual model). Concretely, for \mathcal{D}_t , the LLM is fine-tuned with the standard cross-entropy over the next-item token:

$$L_{\text{ce}}^{\mathcal{D}_t} = \mathbb{E}_{(x,y) \sim \mathcal{D}_t} [-\log p_{\theta}(y | x)], \quad p_{\theta}(y | x) = \text{softmax}(z_{\theta}(x))_y, \quad (2)$$

where $z_{\theta}(x) \in \mathbb{R}^{|\mathcal{V}|}$ are the logits for the item vocabulary \mathcal{V} .

Low-Rank Adaptation (LoRA). LoRA freezes the pretrained LLM weight $W_0 \in \mathbb{R}^{d_{\text{out}} \times d_{\text{in}}}$ and adds a trainable low-rank update:

$$\Delta W = BA, \quad A \in \mathbb{R}^{r \times d_{\text{in}}}, \quad B \in \mathbb{R}^{d_{\text{out}} \times r}, \quad r \ll \min(d_{\text{in}}, d_{\text{out}}), \quad (3)$$

so that for an input $x \in \mathbb{R}^{d_{\text{in}}}$ the layer computes $(W_0 + \Delta W)x$. Only A and B are updated during fine-tuning, while W_0 remains fixed. This yields substantial parameter savings and modular, layer-wise adaptation (e.g., on attention projections). In this work, our analysis and method operate entirely within this LoRA subspace and therefore inherit its efficiency. We now formally define our problem.

Problem 1. (*Continual adaptation of a generative recommender*) **Given:** (1) a pretrained LLM-based recommendation model (fine-tuned with LoRA on \mathcal{D}_1), (2) a sequence of chronological data blocks $\mathcal{D}_2, \dots, \mathcal{D}_T$; **Goal:** learn updates that, at each stage t , adapt the model to \mathcal{D}_t while retaining useful knowledge from earlier stages, achieving high quality next-item recommendation via a balanced stability–plasticity.

3 ANALYSIS OF LoRA VARIANTS FOR CONTINUAL RECOMMENDATION

We introduce two primary baselines for our problem: single evolving LoRA and the cumulative LoRA family. Then, we empirically compare them on a natural chronological split and a user-disjoint split.

Single evolving LoRA. At stage t , the LoRA matrices A_t and B_t are initialized (i.e., parameter inheritance) from the previous stage (A_{t-1} and B_{t-1}) and fine-tuned on new data \mathcal{D}_t :

$$W_t = W_0 + B_t A_t, \quad B_t \leftarrow B_{t-1}, \quad A_t \leftarrow A_{t-1}, \quad (4)$$

¹Adapting the tokenizer to new items over time is an interesting direction; here we fix the item tokenizer to isolate continual adaptation of the model (LoRA).

Table 1: (Left) Design choices; (Right) performance gain vs. single evolving LoRA (w.r.t. NDCG@5) in different task settings on Instrument dataset.

Method	Design choices			Task settings		
	Learnable mag.	Only latest	Param inherit	(1) User-disjoint	(2) Natural split	Diff. (1)-(2)
SUMLoRA _{ALL}	✗	✗	✗	-8.13%	-26.77%	18.64%
SUMLoRA _{LATEST}	✗	✓	✗	-12.20%	-22.05%	9.85%
SUMLoRA _{ALL+INHERIT}	✗	✗	✓	-3.25%	1.57%	-4.82%
SUMLoRA _{LATEST+INHERIT}	✗	✓	✓	0.00%	2.36%	-2.36%
SD-LoRA _{LATEST+INHERIT}	✓	✓	✓	3.25%	0.79%	2.46%

where W_0 is the pretrained LLM weight (i.e., not LoRA updates). This baseline is simple and adapts effectively to new data, while parameter inheritance provides partial preservation of past knowledge at initialization. However, it inevitably overwrites useful past knowledge during fine-tuning, leading to forgetting.

Cumulative LoRA Variants. To mitigate forgetting, cumulative LoRA has been widely used in domains such as vision (Wu et al., 2025; Liang & Li, 2024). At stage t , it reuses frozen adapters from past stages and adds a new trainable adapter by summing them during both training and inference. The effective update is

$$W_t = W_0 + \sum_{i=1}^{t-1} \alpha_i \hat{B}_i \hat{A}_i + B_t A_t, \quad (5)$$

where W_0 is the pretrained LLM weight; $\{\hat{B}_i\}_{i=1}^{t-1}$ and $\{\hat{A}_i\}_{i=1}^{t-1}$ are frozen adapters from previous stages; and B_t, A_t are trainable at stage t . Following prior practice, we use normalized directions $\hat{B}_i = B_i / \|B_i\|_F$ and $\hat{A}_i = A_i / \|A_i\|_F$, which improves stability. The scalar α_i are fixed or learned magnitudes. This design explicitly enhances stability and expands LoRA’s effective capacity, expected to work well when sequential tasks interfere minimally. However, for recommendation where user preferences evolve, this rationale weakens. To examine this, we study SumLoRA, which uses simple summation, in four variants: (i) *all*, summing all past adapters; (ii) *latest*, summing only the most recent adapter; (iii) *all+inherit*, summing all past adapters with parameter inheritance; and (iv) *latest+inherit*, using only the latest adapter with parameter inheritance. The *all* variant corresponds to the original design of cumulative LoRA family. We also consider SD-LoRA, which extends summation with learnable magnitudes, with *all* equivalent to Wu et al. (2025). For analysis, we focus on the empirically stronger *latest+inherit*. Table 1 summarizes these design choices.

Two settings. We evaluate methods in the two settings derived from the same user-item interaction data: (1) **Natural chronological split**: Interactions are sorted by time; a large portion (e.g., 60%) is used for pretraining (i.e., \mathcal{D}_1), and the remainder is divided into four equal incremental blocks, yielding $\mathcal{D}_1, \dots, \mathcal{D}_5$. For each \mathcal{D}_t , we apply leave-one-out per user (second-to-last item for validation, last item for test). See Appendix C.1 for details. (2) **Pseudo user-disjoint split**: Users are randomly partitioned into disjoint sets for \mathcal{D}_t ($t = 1, \dots, 5$), with block sizes matched to the chronological split. Item order within each user’s sequence is preserved. While similar users may induce some shared preferences across stages, this setting introduces relatively less cross-stage interference than the natural chronological case.

Results. Table 1 reports (1) the relative gain vs. single evolving LoRA on the user-disjoint split, (2) the relative gain on the chronological split, and (3) their difference (i.e., (1)-(2)). We summarize the findings: First, the **Diff.** column shows that the original cumulative design (i.e., SUMLoRA_{ALL}) performs much worse in the natural chronological setting than in the user-disjoint setting, confirming that it is better suited for tasks with minimal interference and ill-suited for recommendation. Second, in the **Natural split**, SUMLoRA_{ALL} performs worst, followed by *latest*, *all+inherit*, and *latest+inherit*, suggesting that (a) aggregating all past adapters hinders adaptation, and (b) parameter inheritance is essential for gradual, proximal evolution of LoRA with respect

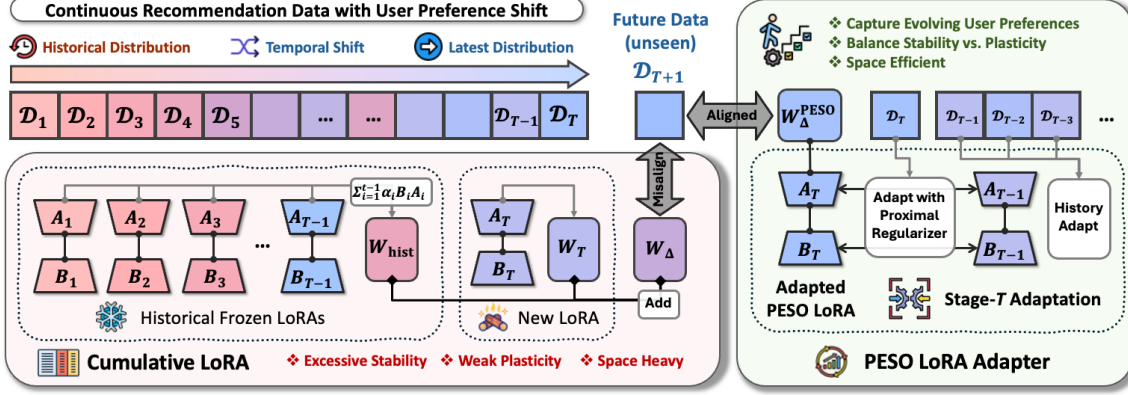


Figure 1: Conceptual overview of Cumulative LoRA and our proposed PESO with proximal regularizer.

to the previous state. Finally, SD-LoRA_{LATEST+INHERIT} fails to improve over fixed-magnitude SUM-LoRA_{LATEST+INHERIT}, since useful past components are entangled with stale ones, making weighting ineffective. Overall, continual recommendation requires evolving adapters with *controlled stability*, rather than rigid reuse of past ones, to capture user preference dynamics.

4 PROPOSED FRAMEWORK: PESO

Our design philosophy is to (1) avoid using multiple LoRA adapters, which implicitly assume task independence, and (2) preserve past knowledge in a way that supports understanding of current user behavior. Guided by this, we propose PESO (Proximally rEgularized Single evolving LoRa), which maintains a single evolving LoRA adapter and regularizes each update by keeping the current adapter close to the previous one (shown in Figure 1). We begin by presenting the *quadratic proximal framework* and its theoretical implications, and then instantiate PESO with a *softmax-KL proximal* to demonstrate its practical effect.

4.1 SINGLE EVOLVING LORA WITH A PROXIMAL REGULARIZER

General framework. We maintain a single evolving LoRA and anchor each update to the previous adapter with a proximal term. Let $v_t \in \mathbb{R}^m$ denote the concatenation of all flattened LoRA A/B parameters at time stage t . We partition coordinates into groups $g \in \{1, \dots, G\}$ (e.g., per module such as attention layers) and write $v^{(g)}$ for group g . The overall loss function for time stage t is

$$L_t = L_{ce}^{\mathcal{D}_t} + \underbrace{\frac{\lambda}{2} \sum_{g=1}^G \|v_t^{(g)} - v_{t-1}^{(g)}\|_{H_{t-1}^{(g)}}^2}_{\text{proximal term}}, \quad v_t \leftarrow v_{t-1} \text{ at init}, \quad (6)$$

where $L_{ce}^{\mathcal{D}_t}$ is the data-fitting term on \mathcal{D}_t (i.e., cross-entropy, Eq. (2)), $\|z\|_H^2 := z^\top H z$, $\lambda > 0$ controls regularization strength, and each $H_{t-1}^{(g)} \succeq 0$ is a (symmetric) PSD metric that is fixed during stage t ; it can be constant (e.g., $H_{t-1}^{(g)} = I$, corresponding to the L2 case) or precomputed at the previous adapter $v_{t-1}^{(g)}$. We initialize $v_t \leftarrow v_{t-1}$ so the proximal penalty starts at zero and grows only as v_t departs from v_{t-1} . This design leverages the natural competition between the data-fitting loss (which pulls toward the optimal state for \mathcal{D}_t) and the proximal term (which pulls toward the previous state). Next, we theoretically show how this yields data-aware, direction-wise guidance in the LoRA subspace.

Theoretical setup. To analyze how the proximal term interacts with the data-fitting loss, we approximate the data-fitting term. We restrict updates to a fixed m -dimensional LoRA subspace. Let $\theta_0 \in \mathbb{R}^d$ be the parameter vector (base LLM and LoRA) after training on the first data block ($t=1$). From $t \geq 2$, let $\theta(v) = \theta_0 + Uv$ with $U \in \mathbb{R}^{d \times m}$ and non-LoRA coordinates frozen (i.e., assume $U = [I_m \ 0]$). For input x = (prompt, item sequence) and next-item token y , let $s(\theta, x)$ be the scalar logit of the ground-truth token. Linearize once at $v = 0$:

$$s(\theta_0 + Uv, x) \approx s(\theta_0, x) + \Phi(x)^\top v, \quad \Phi(x) := U^\top \nabla_\theta s(\theta_0, x) \in \mathbb{R}^m, \quad (7)$$

where $\Phi(x)$ is tangent feature of x . For analysis we use a mean-squared-error surrogate for Eq. (2) and define the stage- t optimum $v_t^* = \arg \min_v L^{\mathcal{D}_t}(v)$. A second-order expansion at v_t^* yields quadratic loss

$$L^{\mathcal{D}_t}(v) \approx \frac{1}{2} (v - v_t^*)^\top \Sigma_t (v - v_t^*), \quad \Sigma_t = \mathbb{E}_{x \sim \mathcal{D}_t} [\Phi(x) \Phi(x)^\top] \succeq 0, \quad (8)$$

where Σ_t is the tangent-feature second-moment matrix for time stage t , capturing *how much the stage- t data supports different directions in the LoRA subspace* (i.e., $u^\top \Sigma_t u = \mathbb{E}_{\mathcal{D}_t}[(\Phi(x)^\top u)^2]$ $\forall u \in \mathbb{R}^m$). See Appendix B.1 for full setup and assumptions. In what follows, we present a general proposition showing that our proximal framework yields direction-wise interpolation between the new optimum and the previous adapter, and then derive its L2 corollary to provide intuition into the stability-plasticity balance.

Proposition 1 (Generalized-eigen interpolation with a quadratic proximal). *Let $\Sigma_t = \Sigma_t^\top \succeq 0$. Define the block-diagonal proximal metric $H_{t-1} := \text{blkdiag}(H_{t-1}^{(1)}, \dots, H_{t-1}^{(G)}) \succeq 0$, with each $H_{t-1}^{(g)}$ symmetric PSD and independent of v during stage t . Under the quadratic approximation in Eq. (8), our loss Eq. (6) is:*

$$L_t(v) = \frac{1}{2} (v - v_t^*)^\top \Sigma_t (v - v_t^*) + \frac{\lambda}{2} (v - v_{t-1})^\top H_{t-1} (v - v_{t-1}). \quad (9)$$

Let $\{(q_k, \rho_k)\}_{k=1}^r$ be generalized eigenpairs of (Σ_t, H_{t-1}) on $\text{range}(H_{t-1})$ (i.e., $\Sigma_t q_k = \rho_k H_{t-1} q_k$), normalized by $q_i^\top H_{t-1} q_j = \delta_{ij}$, where $r = \text{rank}(H_{t-1})$. With $\langle u, w \rangle_{H_{t-1}} := u^\top H_{t-1} w$,

$$\langle v, q_k \rangle_{H_{t-1}} = \frac{\rho_k}{\rho_k + \lambda} \langle v_t^*, q_k \rangle_{H_{t-1}} + \frac{\lambda}{\rho_k + \lambda} \langle v_{t-1}, q_k \rangle_{H_{t-1}}, \quad k = 1, \dots, r. \quad (10)$$

The proof of Proposition 1 is deferred to Appendix B.2. To build intuition, we specialize Proposition 1 to the *L2 case by taking $H_{t-1} = I$* . Then the generalized eigenpairs reduce to ordinary eigenpairs of Σ_t and $\langle \cdot, \cdot \rangle_{H_{t-1}}$ becomes the standard inner product, yielding the following corollary.

Corollary 2 (L2 special case of Proposition 1). *Take $H_{t-1} = I$. If $\Sigma_t q_k = \sigma_k^2 q_k$ with $\{q_k\}$ orthonormal,*

$$\langle v, q_k \rangle = \frac{\sigma_k^2}{\sigma_k^2 + \lambda} \langle v_t^*, q_k \rangle + \frac{\lambda}{\sigma_k^2 + \lambda} \langle v_{t-1}, q_k \rangle, \quad k = 1, \dots, r. \quad (11)$$

In a nutshell, Corollary 2 shows a **data-aware balance between stability and plasticity** in our framework. Recall that $\Sigma_t = \mathbb{E}_{\mathcal{D}_t}[\Phi(x) \Phi(x)^\top]$ summarizes how much the stage- t data supports different directions in the LoRA subspace. Its eigenvectors q_k are principal directions, with eigenvalues σ_k^2 measuring the strength of support along each direction under \mathcal{D}_t . By Corollary 2, along any q_k the update is a weighted average of v_t^* and v_{t-1} , with weight toward v_t^* equal to $\sigma_k^2/(\sigma_k^2 + \lambda)$. Thus, when σ_k^2 is large (strong support in \mathcal{D}_t), v_t moves toward v_t^* along q_k (e.g., the user starts engaging more with mystery than sci-fi); when σ_k^2 is small (weak support), v_t stays close to v_{t-1} (e.g., a stable brand affinity not observed this week). If $\sigma_k^2 = 0$, the component along q_k is kept exactly from the previous stage.

4.2 SOFTMAX–KL AS A PROXIMAL REGULARIZER

As shown earlier, the L2 proximal (i.e., $H_{t-1}^{(g)} = I$) is a special case of our general proximal form with H_{t-1} . However, it penalizes all coordinate changes equally, treating modules uniformly, ignoring internal structure, and not adapting to the previous state v_{t-1} . To address this, we instantiate the proximal term with a *softmax–KL proximal* that preserves per-module structure and leverages the previous state. Formally, the stage- t objective of PESO is:

$$L_t = L_{\text{ce}}^{\mathcal{D}_t} + \lambda \underbrace{\sum_{g=1}^G D_{\text{KL}}(\text{softmax}(v_t^{(g)}) \| \text{softmax}(v_{t-1}^{(g)}))}_{\mathcal{K}_{\text{blk}}(v_t, v_{t-1})}, \quad v_t \leftarrow v_{t-1} \text{ at init.} \quad (12)$$

We first show that the softmax–KL proximal locally reduces to a quadratic form, and then give a corollary that interprets it as a p -weighted variance, providing an intuitive view of its module-wise stability.

Proposition 3 (Per-module softmax–KL is locally quadratic). *Let $v_t^{(g)}$ be the subvector for group $g \in \{1, \dots, G\}$ (e.g., a module), $p^{(g)} = \text{softmax}(v_{t-1}^{(g)})$, and $\Delta^{(g)} = v_t^{(g)} - v_{t-1}^{(g)}$. Then, for small $\Delta^{(g)}$,*

$$\begin{aligned} \mathcal{K}_{\text{blk}}(v_t, v_{t-1}) &= \frac{\lambda}{2} \sum_{g=1}^G (\Delta^{(g)})^\top \left(\text{diag}(p^{(g)}) - p^{(g)} p^{(g)\top} \right) \Delta^{(g)} + o\left(\sum_g \|\Delta^{(g)}\|^2\right) \\ &= \frac{\lambda}{2} \Delta^\top \underbrace{\text{blkdiag}(H_{t-1}^{(1)}, \dots, H_{t-1}^{(G)})}_{=:H_{t-1}} \Delta + o\left(\sum_g \|\Delta^{(g)}\|^2\right), \text{ with } H_{t-1}^{(g)} = \text{diag}(p^{(g)}) - p^{(g)} (p^{(g)})^\top \succeq 0. \end{aligned} \quad (13)$$

The proof of Proposition 3 is deferred to Appendix B.3. Proposition 3 shows the **softmax–KL proximal is locally the quadratic** $\frac{\lambda}{2} \|v_t - v_{t-1}\|_{H_{t-1}}^2$ with $H_{t-1} = \text{blkdiag}(H_{t-1}^{(1)}, \dots, H_{t-1}^{(G)})$. Hence, Proposition 1 applies directly, suggesting it has effect of data-aware balance of stability and plasticity.

Corollary 4 (Softmax–KL equals p -weighted variance). *With notation as above, up to an additive constant,*

$$\mathcal{K}_{\text{blk}}(v_t, v_{t-1}) = \frac{\lambda}{2} \sum_{g=1}^G \text{Var}_{p^{(g)}}(\Delta^{(g)}), \quad \text{Var}_{p^{(g)}}(\Delta^{(g)}) = \sum_{i \in g} p_i^{(g)} (\Delta_i^{(g)} - \mu^{(g)})^2 \text{ and } \mu^{(g)} = \sum_{i \in g} p_i^{(g)} \Delta_i^{(g)}. \quad (14)$$

Corollary 4 shows that, the softmax–KL proximal can be interpreted as a p -weighted variance of parameter changes. Consequently, the proximal (i) penalizes *reshuffling* of weight mass within each module more than uniform shifts, and (ii) protects coordinates with higher prior mass more strongly. **This yields module-wise, previous-state-aware stability** without killing plasticity: updates still move toward new optima where data provides strong support (as in Proposition 1), while staying close to the previous state otherwise.

5 EXPERIMENTS

We design experiments to answer four key questions: **RQ1:** To what extent does PESO outperform competitors? **RQ2:** Which proximal regularizer works best in PESO? **RQ3:** How do hyperparameters affect performance of PESO? **RQ4:** How does PESO compare to traditional continual recommenders?

Table 2: Recommendation performance averaged across time stages for PESO and continual competitors. The best and second-best results are marked in **bold** and underline, respectively.

Methods	Instruments					Movies & TVs					Books		
	H@5	H@10	N@5	N@10	H@5	H@10	N@5	N@10	H@5	H@10	N@5	N@10	
PRETRAIN	0.0166	0.0216	0.0115	0.0131	0.0166	0.0231	0.0111	0.0132	0.0258	0.0283	0.0196	0.0204	
SINGLE EVOLVING LoRA	0.0181	0.0253	0.0127	0.0150	0.0175	0.0247	0.0116	0.0138	0.0448	0.0557	0.0308	0.0344	
Cumulative LoRA Family													
INFLoRA _{ALL}	0.0156	0.0214	0.0105	0.0124	0.0103	0.0139	0.0067	0.0079	0.0236	0.0332	0.0161	0.0193	
INFLoRA _{LATEST}	0.0131	0.0167	0.0090	0.0102	0.0073	0.0092	0.0047	0.0054	0.0152	0.0197	0.0108	0.0123	
INFLoRA _{ALL+INHERIT}	0.0149	0.0219	0.0104	0.0126	0.0109	0.0147	0.0072	0.0085	0.0249	0.0324	0.0171	0.0195	
INFLoRA _{LATEST+INHERIT}	0.0137	0.0202	0.0095	0.0116	0.0094	0.0132	0.0060	0.0072	0.0225	0.0288	0.0153	0.0174	
SUMLoRA _{ALL}	0.0134	0.0215	0.0093	0.0119	0.0102	0.0130	0.0067	0.0076	0.0264	0.0402	0.0176	0.0221	
SUMLoRA _{LATEST}	0.0143	0.0221	0.0099	0.0124	0.0102	0.0130	0.0067	0.0076	0.0246	0.0354	0.0161	0.0196	
SUMLoRA _{ALL+INHERIT}	0.0182	0.0260	0.0129	<u>0.0154</u>	0.0160	0.0234	0.0107	0.0131	0.0409	0.0514	0.0287	0.0321	
SUMLoRA _{LATEST+INHERIT}	0.0185	0.0255	0.0130	0.0152	0.0172	0.0237	0.0114	0.0135	0.0433	0.0542	0.0306	0.0341	
SD-LoRA _{ALL}	0.0156	0.0226	0.0107	0.0129	0.0094	0.0133	0.0061	0.0074	0.0238	0.0351	0.0162	0.0198	
SD-LoRA _{LATEST}	0.0156	0.0218	0.0102	0.0123	0.0101	0.0142	0.0069	0.0082	0.0241	0.0327	0.0159	0.0186	
SD-LoRA _{ALL+INHERIT}	0.0176	0.0238	0.0124	0.0144	0.0118	0.0171	0.0077	0.0094	0.0332	0.0412	0.0234	0.0260	
SD-LoRA _{LATEST+INHERIT}	0.0184	0.0254	0.0128	0.0150	0.0165	0.0235	0.0109	0.0131	0.0432	0.0530	0.0308	0.0340	
PESO	0.0193	0.0268	0.0138	0.0162	0.0180	0.0251	0.0118	0.0141	0.0448	0.0569	0.0311	0.0351	
Performance Gain (%)													
VS. SINGLE EVOLVING LoRA	6.63%	5.93%	8.66%	8.00%	2.86%	1.62%	1.72%	2.17%	0.00%	2.15%	0.97%	2.03%	
VS. SUMLoRA _{LATEST+INHERIT}	4.32%	5.10%	6.15%	6.58%	4.65%	5.91%	3.51%	4.44%	3.46%	4.98%	1.63%	2.93%	
VS. SD-LoRA _{LATEST+INHERIT}	4.89%	5.51%	7.81%	8.00%	9.09%	6.81%	8.26%	7.63%	3.70%	7.36%	0.97%	3.24%	

5.1 EXPERIMENTAL SETTINGS

Datasets. We use the real-world Amazon Review dataset, which contains user reviews (treated as implicit interactions) on products over time. We focus on three categories: Musical Instruments, Movies & TV, and Books. Detailed preprocessing steps and dataset statistics are provided in Appendix C.1. The processed data yield $\{\mathcal{D}_1, \dots, \mathcal{D}_5\}$, where \mathcal{D}_1 is a large pretraining set and $\mathcal{D}_2, \dots, \mathcal{D}_4$ are smaller incremental sets.

Evaluation. For each \mathcal{D}_t , we apply leave-one-out evaluation per user, reserving the last item for testing. Following (Wang et al., 2024; Bao et al., 2025), we construct multiple training pairs (x_u, y_u) per user using a sliding window of size 20. Starting from the LLM pretrained on \mathcal{D}_1 , at each stage $t = 2, \dots, 5$ the model is fine-tuned and then generates 10 items via constrained beam search restricted to valid item tokens. We report Hit@5/10 and NDCG@5/10, averaged over $\mathcal{D}_2, \dots, \mathcal{D}_4$. Full evaluation details are in Appendix C.1.

Compared methods and implementation details. We compare PESO with several LoRA-based baselines for continual learning, all using the same cross-entropy loss and Llama-3.2 1B (Grattafiori et al., 2024) as backbone. The bottom baseline is PRETRAIN, trained on \mathcal{D}_1 and directly evaluated at $t = 2, \dots, 4$. Among continual methods, we consider: (1) *single evolving LoRA*; and (2) the *cumulative family*, which combines past and current adapters: *SumLoRA*, *SD-LoRA* (Wu et al., 2025), and *INFLoRA* (Liang & Li, 2024). SD-LoRA learns magnitudes for normalized past adapters, while INFLoRA precomputes LoRA- A via SVD of the input covariance and trains only B , to better align with current data and reduce task-interference. As discussed in Section 3, original cumulative designs use *all past adapters without inheritance (all)*. For recommendation, we further test three variants: *latest* (most recent only), *all+inherit* (all with inheritance), and *latest+inherit* (latest with inheritance). For hyperparameters, λ is searched over $[0.5, 1.0, 2.0, 5.0, 8.0]$ (set to 2.0 for Instruments, 5.0 for Movies&TV and Books). SD-LoRA magnitudes start at 1.0.

5.2 EXPERIMENTAL RESULTS AND DISCUSSION

Main Results (RQ1). Table 2 reports results across four metrics and three datasets in continual settings. First, all continual learning methods consistently outperform PRETRAIN, highlighting the importance of adapting to new data to capture evolving user preferences, even when incremental data is much smaller (e.g., 10%) than the pretraining data. Second, neither single evolving LoRA nor the cumulative family dominates, while PESO consistently achieves the best results, with average gains of 3.71%, 4.62%, and 6.26% over the best competitors (SINGLE EVOLVING LoRA,



Figure 2: Performance comparison of different regularization methods against the previous LoRA.

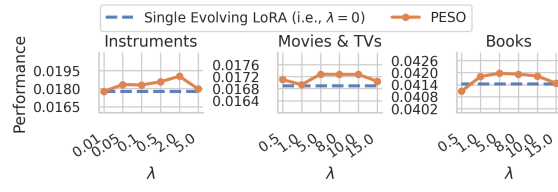


Figure 3: Impact of the scaling weight λ for the proximal term on PESO performance.

$\text{SUMLoRA}_{\text{LATEST+INHERIT}}$, and $\text{SD-LoRA}_{\text{LATEST+INHERIT}}$). Cumulative LoRA, though more complex and storage-heavy, often underperforms or only matches single evolving LoRA, as rigidly reusing frozen adapters overly constrains adaptation to evolving user preferences. By contrast, PESO uses flexible proximal regularization toward the latest state, allowing the data-fitting loss and proximal term to jointly decide what to preserve or update. Third, as discussed in detail in Section 3, regarding SumLoRA and SD-LoRA, original cumulative designs (using all past adapters without inheritance) perform worst, while variants with inheritance or only the latest adapter do better. Notably, some non-inheritance variants even fall below PRETRAIN, showing that without gradual evolution, continual learning can harm more than help. InfLoRA yields the weakest results overall, likely because, although it incorporates input data covariance information, freezing A prevents inheritance and gradual adaptation across time, both of which are crucial in continual recommendation.

Analysis on Proximal Regularizer (RQ2). Unless otherwise noted, all subsequent subsections report average performance across four metrics (Hit@5, Hit@10, NDCG@5, NDCG@10). We compare PESO with four alternative regularizers on the previous adapter: orthogonality, L2 proximal, LoRA-Output KL, and Per-Rank KL (Figure 2). Orthogonality, an interference-minimization strategy common in vision, performs far worse than all methods, showing that minimizing interference across stages is harmful in continual recommendation. L2 proximal, which penalizes the L2 distance between current and previous parameters, is often comparable to single evolving LoRA but worse than PESO, suggesting that uniform constraints are insufficient. LoRA-Output KL (softmax-KL applied in LoRA output, i.e., function space) and Per-Rank KL (softmax-KL applied on each rank of LoRA matrices, i.e., finer parameter granularity) are slightly worse or comparable to PESO, suggesting that regularization directly in the parameter space with module-aware structure is more effective, or at least sufficient, compared to output-level or overly fine-grained constraints.

Hyperparameter Analysis (RQ3). (a) **Scaling parameter λ for proximal term in PESO.** Figure 3 shows performance as λ varies. Starting from $\lambda = 0$ (i.e., single evolving LoRA), performance improves as λ increases, then either decreases or plateaus, confirming that λ serves as a tunable trade-off between stability and plasticity: too small harms stability; too large harms plasticity. In addition, performance is not highly sensitive to λ , as results remain stable across a broad range of values. (b) **Learning rate for continual stages.** See Appendix C.2 for full results and discussion. Since incremental datasets are much smaller than the pretraining set, performance is highly sensitive to learning rate. Our results show that using the pretraining rate leads to overfitting, while scaling the rate down ($\approx 0.05\text{--}0.1\times$) yields the best performance.

Comparison with Traditional Continual Recommeders (RQ4). Details are in Appendix C.3; Table 3 shows a subset (top: traditional, bottom: LLM-based). LLM-based methods generally outperform traditional two-tower models, except on Instruments, where explicit dual modeling of users

Table 3: Comparison of traditional and LLM-based methods.

Method	Instruments	Movies & TVs	Books
Pretrain	0.0153	0.0028	0.0041
Fine-tuning	0.0180	0.0114	0.0218
PISA	0.0194	0.0106	0.0301
Pretrain	0.0157	0.0160	0.0235
Fine-tuning	0.0178	0.0169	0.0414
PESO	0.0190	0.0173	0.0422

and items helps. While PESO achieves higher absolute performance, continual methods like PISA (Yoo et al., 2025) yield larger relative gains in two-tower models, reflecting the advantage of explicit user embeddings in capturing preference drift and the challenge of doing so with LLMs.

6 RELATED WORKS

LLM-based Generative Recommender Systems. Recent advances in large language models (LLMs) have inspired generative approaches to recommendation, where the task is framed as sequence generation. Instead of ranking items from a candidate set, the model autoregressively generates the next item token given a user’s interaction history. Variants of this paradigm includes zero-shot prompting (Lyu et al., 2023), ID-token generation (Tan et al., 2024; Wang et al., 2024), data-efficient fine-tuning (Lin et al., 2024), uncertainty-aware decoding (Kweon et al., 2025), and alignment techniques for recommendation objectives (Cao et al., 2024; Bao et al., 2025; Chen et al., 2024). These works demonstrate that LLMs can flexibly leverage textual and structural signals for recommendation, but they typically assume static data. In contrast, real-world interactions arrive continuously, requiring models that can adapt to evolving user preferences without costly retraining. Our work addresses this gap by studying continual adaptation of generative LLM recommenders.

Continual Learning for Foundational Models and LoRA. Classical continual recommenders use parameter regularization (Xu et al., 2020; Wang et al., 2021; 2023; Yoo et al., 2025), replay buffers (Prabhu et al., 2020; Ahrabian et al., 2021; Zhang et al., 2024b; Zhu et al., 2023), or dynamic architectures (He et al., 2023; Zhang et al., 2023). With large foundational models, parameter-efficient fine-tuning (PEFT) has become central, with LoRA (Hu et al., 2022) as a standard choice. In vision, several continual extensions have been proposed, such as cumulative aggregation of frozen adapters (Liang & Li, 2024; Lu et al., 2024) and learnable magnitude scaling (SD-LoRA) (Wu et al., 2025), which are effective when tasks interference is minimal. However, these methods are less suitable for recommendation, where user preferences evolve over time. Our work differs by proposing a proximal single evolving LoRA that avoids the forgetting of single evolving LoRA and the rigidity of cumulative LoRA, better suiting the continual recommendation setting.

7 CONCLUSION

We have studied the problem of continual adaptation for LLM-based generative recommender systems, where user interactions arrive over time and preferences evolve. Single evolving LoRA offers strong plasticity but suffers from forgetting, while cumulative LoRA improves stability but entangles outdated signals. Our proposed PESO strikes a better balance by maintaining a single adapter and regularizing it toward its prior state, allowing the model to decide what to adapt and what to preserve. Our theoretical analysis has shown that the proximal design provides data-aware, direction-wise guidance in the LoRA subspace, and our instantiation with per-module softmax–KL further preserves internal parameter structure. Empirical results across multiple real-world datasets confirm that PESO consistently outperforms existing baselines, achieving a superior stability–plasticity balance.

Ethics Statement. This work focuses on continual learning methods for large language model (LLM)-based recommender systems. It does not involve human subjects, sensitive personal data, or private user information. All experiments are conducted on publicly available benchmark datasets (Amazon Reviews). We followed standard preprocessing protocols, and no personally identifiable information was used or released. While recommender systems can influence user exposure to content, this study is purely methodological and does not deploy or interact with real users. We acknowledge the potential societal risks of recommendation technologies, such as reinforcing biases or filter bubbles, and we emphasize that our method (PESO) is designed as a modular continual learning technique, independent of any particular application domain or societal factors.

Reproducibility Statement. The paper provides: (1) detailed descriptions of datasets, preprocessing steps, and evaluation protocols (Section 5.1, Appendix C.1); (2) clear definitions of baselines, the proposed method (PESO), and its theoretical analyses (Sections 3, 4, Appendix B); and (3) hyperparameter settings, search ranges, and sensitivity analyses (Section 5). Results are reported across multiple datasets and metrics for robustness. Full proofs are included in Appendix B. We will release our implementation and data-processing scripts upon publication to ensure reproducibility.

REFERENCES

Kian Ahrabian, Yishi Xu, Yingxue Zhang, Jiapeng Wu, Yuening Wang, and Mark Coates. Structure aware experience replay for incremental learning in graph-based recommender systems. In *Proceedings of the 30th ACM International Conference on Information & Knowledge Management*, pp. 2832–2836, 2021.

Elahe Arani, Fahad Sarfraz, and Bahram Zonooz. Learning fast, learning slow: A general continual learning method based on complementary learning system. *arXiv preprint arXiv:2201.12604*, 2022.

Keqin Bao, Jizhi Zhang, Yang Zhang, Wenjie Wang, Fuli Feng, and Xiangnan He. Tallrec: An effective and efficient tuning framework to align large language model with recommendation. In *Proceedings of the 17th ACM conference on recommender systems*, pp. 1007–1014, 2023.

Keqin Bao, Jizhi Zhang, Wenjie Wang, Yang Zhang, Zhengyi Yang, Yanchen Luo, Chong Chen, Fuli Feng, and Qi Tian. A bi-step grounding paradigm for large language models in recommendation systems. *ACM Transactions on Recommender Systems*, 3(4):1–27, 2025.

Yuwei Cao, Nikhil Mehta, Xinyang Yi, Raghunandan Keshavan, Lukasz Heldt, Lichan Hong, Ed H Chi, and Maheswaran Sathiamoorthy. Aligning large language models with recommendation knowledge. *arXiv preprint arXiv:2404.00245*, 2024.

Yuxin Chen, Junfei Tan, An Zhang, Zhengyi Yang, Leheng Sheng, Enzhi Zhang, Xiang Wang, and Tat-Seng Chua. On softmax direct preference optimization for recommendation. *Advances in Neural Information Processing Systems*, 37:27463–27489, 2024.

Jaime Hieu Do and Hady W Lauw. Continual collaborative filtering through gradient alignment. In *Proceedings of the 17th ACM Conference on Recommender Systems*, pp. 1133–1138, 2023.

Aaron Grattafiori, Abhimanyu Dubey, Abhinav Jauhri, Abhinav Pandey, Abhishek Kadian, Ahmad Al-Dahle, Aiesha Letman, Akhil Mathur, Alan Schelten, Alex Vaughan, et al. The llama 3 herd of models. *arXiv preprint arXiv:2407.21783*, 2024.

Bowei He, Xu He, Yingxue Zhang, Ruiming Tang, and Chen Ma. Dynamically expandable graph convolution for streaming recommendation. In *Proceedings of the ACM Web Conference 2023*, pp. 1457–1467, 2023.

Xiangnan He, Kuan Deng, Xiang Wang, Yan Li, Yongdong Zhang, and Meng Wang. Lightgcn: Simplifying and powering graph convolution network for recommendation. In *Proceedings of the 43rd International ACM SIGIR conference on research and development in Information Retrieval*, pp. 639–648, 2020.

Edward J Hu, Yelong Shen, Phillip Wallis, Zeyuan Allen-Zhu, Yuanzhi Li, Shean Wang, Lu Wang, Weizhu Chen, et al. Lora: Low-rank adaptation of large language models. *ICLR*, 1(2):3, 2022.

Wonbin Kweon, Sanghwan Jang, SeongKu Kang, and Hwanjo Yu. Uncertainty quantification and decomposition for llm-based recommendation. In *Proceedings of the ACM on Web Conference 2025*, pp. 4889–4901, 2025.

Yan-Shuo Liang and Wu-Jun Li. Inflora: Interference-free low-rank adaptation for continual learning. In *Proceedings of the IEEE/CVF Conference on Computer Vision and Pattern Recognition*, pp. 23638–23647, 2024.

Xinyu Lin, Wenjie Wang, Yongqi Li, Shuo Yang, Fuli Feng, Yinwei Wei, and Tat-Seng Chua. Data-efficient fine-tuning for llm-based recommendation. In *Proceedings of the 47th International ACM SIGIR Conference on Research and Development in Information Retrieval*, pp. 365–374, 2024.

Xinyu Lin, Haihan Shi, Wenjie Wang, Fuli Feng, Qifan Wang, See-Kiong Ng, and Tat-Seng Chua. Order-agnostic identifier for large language model-based generative recommendation. In *Proceedings of the 48th international ACM SIGIR conference on research and development in information retrieval*, pp. 1923–1933, 2025.

Yuting Liu, Jinghao Zhang, Yizhou Dang, Yuliang Liang, Qiang Liu, Guibing Guo, Jianzhe Zhao, and Xingwei Wang. Cora: Collaborative information perception by large language model’s weights for recommendation. In *Proceedings of the AAAI Conference on Artificial Intelligence*, volume 39, pp. 12246–12254, 2025.

Haodong Lu, Chongyang Zhao, Jason Xue, Lina Yao, Kristen Moore, and Dong Gong. Adaptive rank, reduced forgetting: Knowledge retention in continual learning vision-language models with dynamic rank-selective lora. *arXiv preprint arXiv:2412.01004*, 2024.

Hanjia Lyu, Song Jiang, Hanqing Zeng, Yinglong Xia, Qifan Wang, Si Zhang, Ren Chen, Christopher Leung, Jiajie Tang, and Jiebo Luo. Llm-rec: Personalized recommendation via prompting large language models. *arXiv preprint arXiv:2307.15780*, 2023.

Fei Mi, Xiaoyu Lin, and Boi Faltings. Ader: Adaptively distilled exemplar replay towards continual learning for session-based recommendation. In *Proceedings of the 14th ACM Conference on Recommender Systems*, pp. 408–413, 2020.

Ameya Prabhu, Philip HS Torr, and Puneet K Dokania. Gdumb: A simple approach that questions our progress in continual learning. In *Computer Vision–ECCV 2020: 16th European Conference, Glasgow, UK, August 23–28, 2020, Proceedings, Part II* 16, pp. 524–540. Springer, 2020.

Shashank Rajput, Nikhil Mehta, Anima Singh, Raghunandan Hulikal Keshavan, Trung Vu, Lukasz Heldt, Lichan Hong, Yi Tay, Vinh Tran, Jonah Samost, et al. Recommender systems with generative retrieval. *Advances in Neural Information Processing Systems*, 36:10299–10315, 2023.

Juntao Tan, Shuyuan Xu, Wenyue Hua, Yingqiang Ge, Zelong Li, and Yongfeng Zhang. Idgenre: Llm-recsys alignment with textual id learning. In *Proceedings of the 47th international ACM SIGIR conference on research and development in information retrieval*, pp. 355–364, 2024.

Wenjie Wang, Honghui Bao, Xinyu Lin, Jizhi Zhang, Yongqi Li, Fuli Feng, See-Kiong Ng, and Tat-Seng Chua. Learnable item tokenization for generative recommendation. In *Proceedings of the 33rd ACM International Conference on Information and Knowledge Management*, pp. 2400–2409, 2024.

Yuening Wang, Yingxue Zhang, and Mark Coates. Graph structure aware contrastive knowledge distillation for incremental learning in recommender systems. In *Proceedings of the 30th ACM International Conference on Information & Knowledge Management*, pp. 3518–3522, 2021.

Yuening Wang, Yingxue Zhang, Antonios Valkanas, Ruiming Tang, Chen Ma, Jianye Hao, and Mark Coates. Structure aware incremental learning with personalized imitation weights for recommender systems. In *Proceedings of the AAAI Conference on Artificial Intelligence*, volume 37, pp. 4711–4719, 2023.

Yichen Wu, Hongming Piao, Long-Kai Huang, Renzhen Wang, Wanhua Li, Hanspeter Pfister, Deyu Meng, Kede Ma, and Ying Wei. Sd-lora: Scalable decoupled low-rank adaptation for class incremental learning. *arXiv preprint arXiv:2501.13198*, 2025.

Yishi Xu, Yingxue Zhang, Wei Guo, Hufeng Guo, Ruiming Tang, and Mark Coates. Graphsail: Graph structure aware incremental learning for recommender systems. In *Proceedings of the 29th ACM International Conference on Information & Knowledge Management*, pp. 2861–2868, 2020.

Mao Ye, Ruichen Jiang, Haoxiang Wang, Dhruv Choudhary, Xiaocong Du, Bhargav Bhushanam, Aryan Mokhtari, Arun Kejariwal, and Qiang Liu. Future gradient descent for adapting the temporal shifting data distribution in online recommendation systems. In *Uncertainty in Artificial Intelligence*, pp. 2256–2266. PMLR, 2022.

Hyunsik Yoo, SeongKu Kang, Ruizhong Qiu, Charlie Xu, Fei Wang, and Hanghang Tong. Embracing plasticity: Balancing stability and plasticity in continual recommender systems. In *Proceedings of the 48th International ACM SIGIR conference on research and development in Information Retrieval*, pp. 2092–2101, 2025.

Fajie Yuan, Guoxiao Zhang, Alexandros Karatzoglou, Joemon Jose, Beibei Kong, and Yudong Li. One person, one model, one world: Learning continual user representation without forgetting. In *Proceedings of the 44th International ACM SIGIR Conference on Research and Development in Information Retrieval*, pp. 696–705, 2021.

Kexin Zhang, Yichao Wang, Xiu Li, Ruiming Tang, and Rui Zhang. Incmsr: An incremental learning approach for multi-scenario recommendation. In *Proceedings of the 17th ACM International Conference on Web Search and Data Mining*, pp. 939–948, 2024a.

Peiyan Zhang, Yuchen Yan, Chaozhuo Li, Senzhang Wang, Xing Xie, Guojie Song, and Sunghun Kim. Continual learning on dynamic graphs via parameter isolation. In *Proceedings of the 46th International ACM SIGIR Conference on Research and Development in Information Retrieval*, pp. 601–611, 2023.

Xinni Zhang, Yankai Chen, Chenhao Ma, Yixiang Fang, and Irwin King. Influential exemplar replay for incremental learning in recommender systems. In *Proceedings of the AAAI Conference on Artificial Intelligence*, volume 38, pp. 9368–9376, 2024b.

Jianing Zhu, Jiangchao Yao, Bo Han, Jingfeng Zhang, Tongliang Liu, Gang Niu, Jingren Zhou, Jianliang Xu, and Hongxia Yang. Reliable adversarial distillation with unreliable teachers. *arXiv preprint arXiv:2106.04928*, 2021.

Jieming Zhu, Guohao Cai, Junjie Huang, Zhenhua Dong, Ruiming Tang, and Weinan Zhang. Reloop2: Building self-adaptive recommendation models via responsive error compensation loop. In *Proceedings of the 29th ACM SIGKDD Conference on Knowledge Discovery and Data Mining*, pp. 5728–5738, 2023.

A CONCEPTUAL MODELING OF EVOLVING USER PREFERENCES

We assume an initial model is pretrained offline on base data \mathcal{D}_1 , and then fine-tuned sequentially on chronologically arriving blocks $\mathcal{D}_2, \dots, \mathcal{D}_T$. Let x_u^{t-1} denote u 's interaction history available before stage t , and let $P_t(y | x_u^{t-1})$ be the conditional distribution of the next item y during stage t , representing user preferences. In continual recommendation, these distributions evolve over time, which can be conceptually modeled as

$$P_t(y | x_u^{t-1}) \approx \alpha_t P_{t-1}(y | x_u^{t-1}) + (1 - \alpha_t) Q_t(y | x_u^{t-1}), \quad (15)$$

where P_{t-1} captures stability (persistent long-term preferences), Q_t captures plasticity (new or shifting preferences estimated from new data), and $\alpha_t \in [0, 1]$ controls the balance. The goal is to minimize expected risk on upcoming interactions by balancing stability and plasticity.

B DETAILED THEORETICAL ANALYSIS

B.1 SETUP AND ASSUMPTIONS

Assumption 1 (Parameters and LoRA subspace). *Let $\theta \in \mathbb{R}^d$ denote the vectorized concatenation of all model parameters (base LLM and LoRA). Let θ_0 be the parameter vector after training on the first data block ($t=1$). From $t \geq 2$, restrict updates to a fixed m -dimensional LoRA subspace spanned by columns of $U \in \mathbb{R}^{d \times m}$ and write*

$$\theta = \theta_0 + Uv, \quad v \in \mathbb{R}^m, \quad (16)$$

with all non-LoRA coordinates frozen. Without loss of generality, assume $U = [I_m \ 0]$, i.e., the LoRA subspace is the first m coordinates.

Assumption 2 (Linearization and tangent features.). *Let $s(\theta, x) \in \mathbb{R}$ be the scalar logit of the ground-truth next item. We linearize s at $v = 0$ (i.e., at $\theta = \theta_0$):*

$$s(\theta_0 + v, x) \approx s(\theta_0, x) + v^\top U^\top \nabla_{\theta} s(\theta_0, x) = s_0(x) + v^\top \Phi(x), \quad (17)$$

with tangent features of x

$$\Phi(x) := U^\top \nabla_{\theta_{1:m}} s(\theta_0, x) \in \mathbb{R}^m. \quad (18)$$

Assumption 3 (Data and loss.). *Let $(x, y) \sim \mathcal{D}_t$ be examples in block t . In recommendation, $x = (\text{prompt, item sequence})$ and $y \in \mathcal{V}$ is the next-item token. Training typically uses cross-entropy on logits; for analysis, we use a mean-squared-error (MSE) surrogate. Define the block- t risk*

$$L^{\mathcal{D}_t}(v) = \mathbb{E}_{(x,y) \sim \mathcal{D}_t} \left[\frac{1}{2} (s(\theta_0 + v, x) - r_t(x, y))^2 \right]. \quad (19)$$

where $r_t(x, y) \in \mathbb{R}$ is a calibrated target score for the ground-truth next item.

Note that under the linearization, this yields a quadratic risk with positive-semidefinite curvature. All later proofs use only this PSD curvature, not the exact form of r_t .

Assumption 4 (Quadratic form under the linearization.). *Substituting $s(\theta_0 + v, x) \approx s_0(x) + \Phi(x)^\top v$ gives, up to an additive constant,*

$$L^{\mathcal{D}_t}(v) = b_t^\top v + \frac{1}{2} v^\top \Sigma_t v, \quad b_t := \mathbb{E}_{\mathcal{D}_t} [(s_0(x) - r_t(x, y)) \Phi(x)], \quad \Sigma_t := \mathbb{E}_{\mathcal{D}_t} [\Phi(x) \Phi(x)^\top] \succeq 0. \quad (20)$$

Define the block- t optimum

$$v_t^* = \arg \min_v L^{\mathcal{D}_t}(v). \quad (21)$$

A second-order Taylor expansion of L_t at v_t^* gives

$$L^{\mathcal{D}_t}(v) = L^{\mathcal{D}_t}(v_t^*) + \underbrace{(\nabla L^{\mathcal{D}_t})^\top(v_t^*)(v - v_t^*)}_{=0} + \frac{1}{2}(v - v_t^*)^\top \underbrace{\nabla^2 L^{\mathcal{D}_t}(v_t^*)}_{=\Sigma_t}(v - v_t^*). \quad (22)$$

Dropping the constant term, the centered quadratic risk used throughout is

$$L^{\mathcal{D}_t}(v) = \frac{1}{2}(v - v_t^*)^\top \Sigma_t(v - v_t^*), \quad (23)$$

where Σ_t is the tangent-feature second-moment matrix for time stage t , capturing *how much the stage- t data supports different directions in the LoRA subspace* (i.e., $u^\top \Sigma_t u = \mathbb{E}_{\mathcal{D}_t}[(\Phi(x)^\top u)^2]$ $\forall u \in \mathbb{R}^m$). Also note that we fix the linearization at θ_0 : $s(\theta_0 + Uv, x) \approx s_0(x) + \Phi(x)^\top v$ with $\Phi(x) = U^\top \nabla_\theta s(\theta_0, x)$. Although $\Phi(x)$ is fixed across t , the $\Sigma_t = \mathbb{E}_{\mathcal{D}_t}[\Phi(x)\Phi(x)^\top]$ varies with the data block distribution, so drift is captured via Σ_t and the shifting optimum v_t^* .

Remark: relinearization per block. If desired, one may instead relinearize at $\theta_0 + Uv_{t-1}$, replacing $\Phi(x)$ by $\Phi_{t-1}(x) = U^\top \nabla_\theta s(\theta_0 + Uv_{t-1}, x)$ and Σ_t by $\mathbb{E}[\Phi_{t-1}\Phi_{t-1}^\top]$. All propositions and closed forms carry over with these substitutions; the only change is that the curvature reflects the anchor v_{t-1} of the current block. We found fixed linearization sufficient and notationally lighter.

B.2 PROOF OF PROPOSITION 1.

Assumption 5 (Complementarity (no doubly-flat directions)). *On the LoRA subspace \mathbb{R}^m , let $\Sigma_t \succeq 0$ and $H \succeq 0$ be symmetric (and fixed w.r.t. v). Assume*

$$\ker(\Sigma_t) \cap \ker(H) = \{0\}. \quad (24)$$

Equivalently, for all $x \neq 0$, $x^\top \Sigma_t x > 0$ or $x^\top H x > 0$.

Proof. (i) Differentiate:

$$\nabla_v \mathcal{L}_t(v) = \Sigma_t(v - v_t^*) + \lambda H_{t-1}(v - v_{t-1}). \quad (25)$$

Setting the gradient to zero gives the normal equation

$$(\Sigma_t + \lambda H_{t-1})v = \Sigma_t v_t^* + \lambda H_{t-1} v_{t-1}. \quad (26)$$

For any $x \neq 0$,

$$x^\top (\Sigma_t + \lambda H_{t-1})x = x^\top \Sigma_t x + \lambda x^\top H_{t-1} x \geq 0. \quad (27)$$

Equality forces $x \in \ker(\Sigma_t) \cap \ker(H_{t-1})$, which is $\{0\}$ by Assumption 5; hence $\Sigma_t + \lambda H_{t-1} \succ 0$. Therefore Eq. (26) has the unique solution

$$v = (\Sigma_t + \lambda H_{t-1})^{-1}(\Sigma_t v_t^* + \lambda H_{t-1} v_{t-1}). \quad (28)$$

(ii) Let (q_k, ρ_k) be any generalized eigenpair on $\text{range}(H_{t-1})$ with $q_i^\top H_{t-1} q_j = \delta_{ij}$ and $\Sigma_t q_k = \rho_k H_{t-1} q_k$. Left-multiply Eq. (26) by q_k^\top and use symmetry of Σ_t, H_{t-1} :

$$q_k^\top \Sigma_t v + \lambda q_k^\top H_{t-1} v = q_k^\top \Sigma_t v_t^* + \lambda q_k^\top H_{t-1} v_{t-1}. \quad (29)$$

Since $\Sigma_t q_k = \rho_k H_{t-1} q_k$ and $\langle u, w \rangle_{H_{t-1}} = u^\top H_{t-1} w$,

$$(\rho_k + \lambda) \langle v, q_k \rangle_{H_{t-1}} = \rho_k \langle v_t^*, q_k \rangle_{H_{t-1}} + \lambda \langle v_{t-1}, q_k \rangle_{H_{t-1}}, \quad (30)$$

which yields the stated interpolation.

(iii) **Note on $\ker(H_{t-1})$.** If $H_{t-1} \succ 0$, then $r = m$ and (ii) covers all directions. If H_{t-1} is singular, the interpolation is stated on $\text{range}(H_{t-1})$; along $\ker(H_{t-1})$, $q^\top H_{t-1}(\cdot) \equiv 0$, and the complementarity assumption rules out underdetermined (doubly-flat) directions, ensuring uniqueness. \square

B.3 PROOF OF PROPOSITION 3

To prove Proposition 3, we first establish the following proposition for arbitrary v_t and v_{t-1} , and then extend it to the blockwise case.

Proposition 5 (Local quadratic form of softmax-KL proximal). *Let $p := \text{softmax}(v_{t-1}) \in \mathbb{R}^d$ and $\Delta := v_t - v_{t-1}$. Define*

$$\mathcal{K}(\Delta) := D_{\text{KL}}(\text{softmax}(v_{t-1} + \Delta) \parallel \text{softmax}(v_{t-1})). \quad (31)$$

Then $\mathcal{K}(0) = 0$, $\nabla \mathcal{K}(0) = 0$, and the second-order Taylor expansion at $\Delta = 0$ is

$$\mathcal{K}(\Delta) = \frac{1}{2} \Delta^\top (\text{diag}(p) - pp^\top) \Delta + o(\|\Delta\|^2). \quad (32)$$

Equivalently,

$$\mathcal{K}(\Delta) = \frac{1}{2} \underbrace{\left(\sum_{i=1}^d p_i (\Delta_i - \mu)^2 \right)}_{\text{Var}_p(\Delta)} + o(\|\Delta\|^2), \quad \mu := \sum_{i=1}^d p_i \Delta_i. \quad (33)$$

Proof. Write $r(\Delta) := \text{softmax}(v_{t-1} + \Delta) \in \mathbb{R}^d$ and $p := r(0) = \text{softmax}(v_{t-1})$. By definition,

$$\mathcal{K}(\Delta) = \sum_{i=1}^d r_i(\Delta) \log \frac{r_i(\Delta)}{p_i}. \quad (34)$$

(i) At $\Delta = 0$ we have $r(0) = p$, so

$$\mathcal{K}(0) = \sum_i p_i \log(p_i/p_i) = 0. \quad (35)$$

For the gradient, differentiate using the scalar identity $\frac{d}{dx} [x \log(x/c)] = \log(x/c) + 1$:

$$\frac{\partial \mathcal{K}}{\partial \Delta_a} = \sum_{i=1}^d \frac{\partial r_i}{\partial \Delta_a} \left(\log \frac{r_i}{p_i} + 1 \right). \quad (36)$$

Evaluating at $\Delta = 0$ gives $\log(r_i/p_i) = 0$ and hence

$$\left[\nabla \mathcal{K}(0) \right]_a = \sum_{i=1}^d \left[\frac{\partial r_i}{\partial \Delta_a} \right]_{\Delta=0} = \frac{\partial}{\partial \Delta_a} \left(\sum_{i=1}^d r_i(\Delta) \right) \Big|_{\Delta=0} = \frac{\partial}{\partial \Delta_a} (1) = 0, \quad (37)$$

since softmax outputs sum to one for all Δ .

(ii) Differentiate the gradient once more:

$$\frac{\partial^2 \mathcal{K}}{\partial \Delta_a \partial \Delta_b} = \sum_{i=1}^d \frac{\partial^2 r_i}{\partial \Delta_a \partial \Delta_b} \left(\log \frac{r_i}{p_i} + 1 \right) + \sum_{i=1}^d \frac{\partial r_i}{\partial \Delta_a} \frac{1}{r_i} \frac{\partial r_i}{\partial \Delta_b}. \quad (38)$$

At $\Delta = 0$, the first sum becomes $\sum_i \partial^2 r_i / \partial \Delta_a \partial \Delta_b$ (since $\log(r_i/p_i) = 0$), which is zero because $\sum_i r_i(\Delta) \equiv 1$ for all Δ . Thus,

$$\left[\nabla^2 \mathcal{K}(0) \right]_{ab} = \sum_{i=1}^d \frac{1}{p_i} \left[\frac{\partial r_i}{\partial \Delta_a} \right]_{\Delta=0} \left[\frac{\partial r_i}{\partial \Delta_b} \right]_{\Delta=0}. \quad (39)$$

It remains to compute the Jacobian of softmax at v_{t-1} :

$$J_{ia} := \left[\frac{\partial r_i}{\partial \Delta_a} \right]_{\Delta=0} = \frac{\partial}{\partial v_a} \left(\frac{e^{v_i}}{\sum_j e^{v_j}} \right) \Big|_{v=v_{t-1}} = p_i (\mathbf{1}\{i=a\} - p_a). \quad (40)$$

Therefore,

$$\left[\nabla^2 \mathcal{K}(0) \right]_{ab} = \sum_{i=1}^d \frac{1}{p_i} J_{ia} J_{ib} = \sum_{i=1}^d p_i (\mathbf{1}\{i=a\} - p_a) (\mathbf{1}\{i=b\} - p_b). \quad (41)$$

Expanding the sum gives

$$\sum_i p_i \mathbf{1}\{i=a\} \mathbf{1}\{i=b\} - p_b \sum_i p_i \mathbf{1}\{i=a\} - p_a \sum_i p_i \mathbf{1}\{i=b\} + p_a p_b \sum_i p_i. \quad (42)$$

Since $\sum_i p_i = 1$ and $\sum_i p_i \mathbf{1}\{i=a\} = p_a$, this equals

$$\delta_{ab} p_a - p_a p_b - p_a p_b + p_a p_b = \delta_{ab} p_a - p_a p_b, \quad (43)$$

i.e.

$$\nabla^2 \mathcal{K}(0) = \text{diag}(p) - pp^\top. \quad (44)$$

(iii) By Taylor's theorem,

$$\mathcal{K}(\Delta) = \frac{1}{2} \Delta^\top (\text{diag}(p) - pp^\top) \Delta + o(\|\Delta\|^2). \quad (45)$$

Finally, note the algebraic identity (weighted variance):

$$\Delta^\top (\text{diag}(p) - pp^\top) \Delta = \sum_{i=1}^d p_i \Delta_i^2 - \left(\sum_{i=1}^d p_i \Delta_i \right)^2 = \sum_{i=1}^d p_i (\Delta_i - \mu)^2, \quad \mu := \sum_{i=1}^d p_i \Delta_i. \quad (46)$$

□

Now we prove Proposition 3. Since the blockwise softmax-KL regularizer acts independently on each group g ,

$$\mathcal{K}_{\text{blk}}(\Delta) = \sum_{g=1}^G D_{\text{KL}}(\text{softmax}(v_{t-1}^{(g)} + \Delta^{(g)}) \parallel \text{softmax}(v_{t-1}^{(g)})), \quad (47)$$

with $\mathcal{K}^{(g)}$ defined on group g . Applying Proposition 5 to each group yields block Hessians

$$H^{(g)} = \text{diag}(p^{(g)}) - p^{(g)}(p^{(g)})^\top, \quad (48)$$

which assemble into the block-diagonal

$$H = \text{blockdiag}(H^{(1)}, \dots, H^{(G)}). \quad (49)$$

The variance identity holds within each group.

Table 4: Dataset statistics.

	Total Users	New Users	Total Items	New Items	Total Interactions	Avg Seq Len	Sparsity
Instruments	\mathcal{D}_1	17,046	17,046	40,471	40,471	141,788	8.32 0.9998
	\mathcal{D}_2	1,772	1,183	8,346	2,900	13,197	7.45 0.9991
	\mathcal{D}_3	1,821	1,265	8,325	2,909	13,334	7.32 0.9991
	\mathcal{D}_4	2,289	1,684	9,617	3,864	18,811	8.22 0.9991
	\mathcal{D}_5	2,238	1,699	9,131	3,365	17,573	7.85 0.9991
	$\mathcal{D}_{1:5}$	22,877	NA	53,509	NA	204,703	NA NA
Movies & TVs	\mathcal{D}_1	17,928	17,928	39,228	39,228	190,411	10.62 0.9997
	\mathcal{D}_2	1,866	1,141	11,612	1,479	17,665	9.47 0.9992
	\mathcal{D}_3	2,106	1,200	12,658	1,926	19,874	9.44 0.9993
	\mathcal{D}_4	2,284	1,357	13,788	1,882	22,929	10.04 0.9993
	\mathcal{D}_5	2,332	1,552	13,491	1,559	22,225	9.53 0.9993
	$\mathcal{D}_{1:5}$	23,178	NA	46,074	NA	273,104	NA NA
Books	\mathcal{D}_1	15,406	15,406	35,984	35,984	164,858	10.7 0.9997
	\mathcal{D}_2	1,807	618	7,155	2,711	13,918	7.7 0.9989
	\mathcal{D}_3	1,672	619	6,484	2,278	12,395	7.41 0.9989
	\mathcal{D}_4	1,948	650	7,154	2,657	14,824	7.61 0.9989
	\mathcal{D}_5	1,652	1,025	5,913	2,274	11,990	7.26 0.9988
	$\mathcal{D}_{1:5}$	18,318	NA	45,904	NA	217,985	NA NA

C EXPERIMENTS

C.1 EXPERIMENTAL SETUP

Datasets. We use the real-world temporal Amazon Review dataset, which contains user reviews (treated as implicit interactions) on Amazon products over time.² We focus on three categories: Musical Instruments, Movies & TV, and Books. For Instruments and Movies & TV, we use data from 2019–2023; for Books, we use 2022–2023. We take 60% of the data as pretraining \mathcal{D}_1 and split the remaining 40% into four equal incremental stages, $\mathcal{D}_2, \dots, \mathcal{D}_5$. For each incremental stage, we filter out users with fewer than five interactions. This ensures leave-one-out evaluation is feasible and makes incremental data even smaller than pretraining data, simulating real-world scenarios. Table 4 summarizes dataset statistics, including the number of users, items, and interactions at each stage, average sequence length, and sparsity.

Evaluation. For each \mathcal{D}_t , we apply leave-one-out per user: the second-to-last item is used for validation and the last item is reserved for testing. Following prior work (Wang et al., 2024; Bao et al., 2025), we construct multiple training pairs (x_u, y_u) per user u using a sliding window of size 20. The LLM trained on \mathcal{D}_1 serves as the pretrained model for all compared methods. At each stage $t = 2, \dots, 5$, after fine-tuning, the LLM autoregressively generates 10 items given the user history in the test pair. Generation uses constrained beam search restricted to valid item tokens, making it efficient and widely adopted in prior work (Wang et al., 2024; Rajput et al., 2023). With these 10 items, we evaluate against the ground-truth item and report Hit@5, Hit@10, NDCG@5, and NDCG@10, averaged over $\mathcal{D}_2, \dots, \mathcal{D}_4$.

Metrics. Hit@ k measures whether the ground-truth item appears among the k generated items. For a user u with ground-truth item y_u and a ranked list of predictions R_u ,

$$\text{Hit}@k(u) = \begin{cases} 1 & \text{if } y_u \in R_u[1 : k], \\ 0 & \text{otherwise.} \end{cases}$$

²<https://amazon-reviews-2023.github.io/>

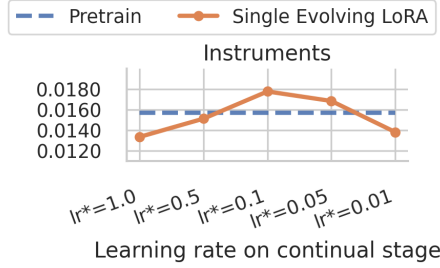


Figure 4: Impact of the learning rate for continual data on model performance.

Table 5: Comparison of LLM-based and traditional methods in continual recommendation.

		Instruments	Movies & TVs	Books
Traditional two-tower	Pretrain	0.0153	0.0028	0.0041
	Fine-tuning	0.0180	0.0114	0.0218
	Contrastive	0.0177	0.0101	0.0272
	Contrastive + PIW	0.0193	0.0113	0.0243
	PISA	0.0194	0.0106	0.0301
LLM-based	Pretrain	0.0157	0.0160	0.0235
	Fine-tuning (w/ LoRA)	0.0178	0.0169	0.0414
	PESO	0.0190	0.0173	0.0422

NDCG@k (Normalized Discounted Cumulative Gain) additionally accounts for the position of the ground-truth item, giving higher credit when it appears closer to the top:

$$\text{NDCG}@k(u) = \begin{cases} \frac{1}{\log_2(\text{rank}(y_u)+1)} & \text{if } y_u \in R_u[1:k], \\ 0 & \text{otherwise,} \end{cases}$$

Hit@k captures whether the correct item is recommended at all, while *NDCG@k* rewards ranking it higher in the list. We report averages of *Hit@k* and *NDCG@k* across all users, with $k \in 5, 10$.

C.2 LEARNING RATE ON CONTINUAL STAGE

Incremental datasets are much smaller than the pretraining set \mathcal{D}_1 (see Appendix C.1), making performance sensitive to learning rate. Figure 4 shows results for single evolving LoRA with varying learning rates on incremental data. Using the pretraining rate (0.001; $lr^*=1.0$) performs worse than not learning new data, likely due to overfitting. The best performance occurs with $lr^*=0.05-0.1$, which aligns with the relative block size $|\mathcal{D}_t|/|\mathcal{D}_1| \approx 0.1$. This suggests that learning rates for incremental blocks should be scaled with respect to data size.

C.3 COMPARISON WITH TRADITIONAL CONTINUAL RECOMMENDER SYSTEMS

We compare our LLM-based methods (pretrain, single evolving LoRA, and PESO) against two-tower methods with LightGCN (He et al., 2020) as backbone, including Pretrain, Fine-tuning, Contrastive (Wang et al., 2021), Contrastive+PIW (Wang et al., 2023), and PISA (Yoo et al., 2025). Two-tower models use explicit user and item embeddings, and their continual methods

mitigate forgetting by regularizing user embeddings against past versions: Contrastive maximizes mutual information between past and current embeddings, Contrastive+PIW further adapts the regularization weights per user, and PISA combines stability and plasticity regularization.

Table 5 reports results averaged across time stages and metrics. First, LLM-based recommenders (both pretrain and continual) generally outperform traditional methods, highlighting the generalization ability and knowledge transfer benefits of LLMs. On Instruments, however, the performance gap is smaller, suggesting that explicit dual modeling of users and items still provides benefits for capturing collaborative signals. It is worth noting that there also remains considerable headroom for LLM-based models if larger beam sizes are used during generation.

Second, While PESO outperforms traditional continual methods in absolute terms, the relative gains of continual techniques over their respective pretraining baselines are larger in traditional settings. This is likely because two-tower methods explicitly capture preference shifts through user embeddings, supporting our view that modeling user preference drift is crucial in continual recommendation. At the same time, it underscores the difficulty of capturing such dynamics in LLM-based methods, pointing to an important direction for future research.

D PROMPT

We show below the template used in all experiments. Notably, `<a_[i1]><b_[j1]><c_[k1]><d_[l1]>` represents one user-item interaction encoded as four semantic-ID tokens. For instance, `<a_144><b_72><c_103><d_217>` is one such tuple describing a single interacted item (Rajput et al., 2023; Wang et al., 2024).

```
Below is an instruction that describes a task.
Write a response that appropriately completes the request.\n\n

### Instruction:\n
Based on the items that the user has interacted with:
<a_[i1]><b_[j1]><c_[k1]><d_[l1]>,
<a_[i2]><b_[j2]><c_[k2]><d_[l2]>,
...
<a_[iN]><b_[jN]><c_[kN]><d_[lN]>,
can you determine what item would be recommended to the user next?\n\n

### Response:
```

E USE OF LARGE LANGUAGE MODELS

LLMs were used only for writing polish (grammar and clarity). All content was reviewed and approved by the authors. LLMs did not contribute to research ideation, algorithm design, implementation, or analysis.